E. coli Expression of TIMP-4 and Comparative Kinetic Studies with TIMP-1 and TIMP-2: Insights into the Interactions of TIMPs and Matrix Metalloproteinase 2 (Gelatinase A)†

Linda Troeberg,‡ Mitsuo Tanaka,§ Robin Wait,‡ Yeunian E. Shi,|| Keith Brew,⊥ and Hideaki Nagase*,‡,§

Kennedy Institute of Rheumatology Division, Imperial College of Science, Technology and Medicine, 1 Aspenlea Road, Hammersmith, London, W6 8LH U.K., Department of Biochemistry and Molecular Biology, University of Kansas Medical Centre, Kansas City, Kansas 66160, Long Island Jewish Medical Centre, The Long Island Campus for the Albert Einstein College of Medicine, New Hyde Park, New York 11040, and Department of Biomedical Sciences, Florida Atlantic University, Boca Raton, Florida 33431

Received July 15, 2002; Revised Manuscript Received August 30, 2002

ABSTRACT: The inhibitory properties of TIMP-4 for matrix metalloproteinases (MMPs) were compared to those of TIMP-1 and TIMP-2. Full-length human TIMP-4 was expressed in *E. coli*, folded from inclusion bodies, and the active component was purified by MMP-1 affinity chromatography. Progress curve analysis of MMP inhibition by TIMP-4 indicated that association rate constants (k_{on}) and inhibition constants (K_i) were similar to those for other TIMPs ($\sim 10^5$ M^{-1} s^{-1} and $10^{-9}-10^{-12}$ M, respectively). Dissociation rate constants (k_{off}) for MMP-1 and MMP-3 determined using α_2-macroglobulin to capture MMP dissociating from MMP-TIMP complexes were in good agreement with values deduced from progress curves ($\sim 10^{-4}$ s^{-1}). K_i and k_{on} for the interactions of TIMP-1, -2, and -4 with MMP-1 and -3 were shown to be pH dependent. TIMP-4 retained higher reactivity with MMPs at more acidic conditions than either TIMP-1 or TIMP-2. Molecular interactions of TIMPs and MMPs investigated by IAsys biosensor analysis highlighted different modes of interaction between proMMP-2-TIMP-2 (or TIMP-4) and active MMP-2-TIMP-2 (or TIMP-4) complexes. The observation that both active MMP-2 and inactive MMP-2 (with the active site blocked either by the propeptide or a hydroxamate inhibitor) have essentially identical affinities for TIMP-2 suggests that there are two TIMP binding sites on the hemopexin domain of MMP-2: one with high affinity that is involved in proMMP-2 or hydroxamate-inhibited MMP-2; and the other with low affinity involved in formation of the complex of active MMP-2 and TIMP-2. Similar models of interaction may apply to TIMP-4. The latter low-affinity site functions in conjunction with the active site of MMP-2 to generate a tight enzyme−inhibitor complex.

Tissue inhibitors of metalloproteinases (TIMPs)[1] are important regulators of extracellular matrix turnover as primary inhibitors of matrix metalloproteinase (MMP) activity within tissues. The four known mammalian TIMPs are homologues consisting of two distinct domains, each containing three disulfide bonds (*1*, *2*). The α-amino and carbonyl groups of the TIMP N-terminal half-cystine mediate inhibition by coordinating the catalytic zinc ion of the target MMP (*1*, *2*). Previous studies have indicated that TIMPs differ in their affinity for various MMPs, as well as in their expression profiles, tissue localization, and ability to bind to MMP zymogens (*1*, *2*). TIMP-1 and TIMP-2 bind to the C-terminal hemopexin-like domains (HPX) of proMMP-9 and proMMP-2, respectively (*3*, *4*). The in vivo role of TIMP-1-proMMP-9 binding is unknown, but TIMP-2 binding to proMMP-2 is required for activation of the zymogen by cell surface-bound MT1-MMP (*5*−*7*). TIMP-4 is also able to bind to proMMP-2, but cannot support its activation by MT1-MMP (*8*−*11*).

TIMP-2 is constitutively and widely expressed, while TIMP-1 and TIMP-3 expression is increased in response to signals such as cytokines, hormones, and mitogens (*12*−*16*). TIMP-4 differs from other members of the family in being expressed at highest levels in the heart (*17*, *18*), where it may protect against cardiomyopathy, tumor development, and metastasis (*19*). Lower levels of TIMP-4 expression are seen in kidney, placenta, and testes (*17*), and TIMP-4 is up-regulated in response to vascular injury (*20*) and in certain cancers (*21*−*25*).

TIMP-4 has highest sequence identity to TIMP-2 [51% identical, 70% similar (*17*)], with both having an extended loop between the A and B β-strands of the N-terminal domain that is not present in TIMP-1 or TIMP-3 (*26*−*29*). The role of this loop in TIMP-4 specificity is currently unknown, but site-directed mutagenesis (*30*) and NMR (*28*)

† This work was supported by Wellcome Trust Grant No. 057508 and NIH Grant AR40994.

* Corresponding author. Phone: +44-(0)20-8383 4488. Fax: +44-(0)20-8563 0399. E-mail: h.nagase@ic.ac.uk.

‡ Imperial College of Science, Technology and Medicine.

§ University of Kansas Medical Centre.

|| Long Island Jewish Medical Centre.

⊥ Florida Atlantic University.

[1] Abbreviations: α_2M, α_2-macroglobulin; APMA, 4-aminophenylmercuric acetate; ΔC, lacking C-terminal hemopexin domain; HPX, hemopexin domain; HPX_{MMP-2}, hemopexin domain of MMP-2; MMP, matrix metalloproteinase; MT, membrane-type; TIMP, tissue inhibitor of metalloproteinases.

10.1021/bi026454l CCC: $22.00
Published on Web 11/16/2002

studies of TIMP-2 indicate that this mobile loop affects the affinity of TIMP-2 for various MMPs.

Here we report functional characterization of full-length human TIMP-4 expressed in *Escherichia coli* and folded from inclusion bodies. On the basis of K_i and k_{on} data, TIMP-4 is broadly similar to other TIMPs in terms of its affinity for various MMPs. However, TIMP-4 retains activity at more acidic pHs than TIMP-1 or TIMP-2. In addition, IAsys biosensor analysis has provided new insights into the interaction between proMMP-2/MMP-2 and TIMPs.

EXPERIMENTAL PROCEDURES

Expression of TIMPs and MMPs. Recombinant proMMP-1 and C-terminally truncated human proMMP-1 [proMMP-1(ΔC)] were expressed in *E. coli* and purified as previously described (*31*). These were activated to generate MMP-1 and MMP-1(Δ*C*) using 1 mM 4-aminophenylmercuric acetate (APMA, ICN Biochemicals, Costa Mesa, CA) and MMP-3(ΔC) [10:1 molar ratio of proMMP-1:MMP-3(ΔC); 90 min at 37 °C (*32*)]. MMP-3(Δ*C*) was removed from activated MMP-1 and MMP-1(ΔC) using an anti-MMP-3 immunoaffinity column (*33*). ProMMP-2 was purified from human uterine cervical fibroblasts (*34*) and activated immediately prior to use by incubation with 1 mM APMA for 1 h at 37 °C. These conditions produced stable, full-length 65 kDa MMP-2 that contained no observable zymogen, 45 kDa, or other auto-catalytic cleavage products. Recombinant HPX_{MMP-2} was prepared by over-activation of proMMP-2 (1 mM APMA, 24 h, 37 °C) and purified by gel filtration. Recombinant C-terminally truncated human proMMP-3 [proMMP-3(ΔC)] was expressed in *E. coli*, purified as described previously (*35*), and activated with 1 mM APMA (*32*). ProMMP-3 was expressed in *E. coli*, purified as described (*31*), and activated using 100 ng/mL chymotrypsin (Sigma-Aldrich, St. Louis, MO) (*31*). Pro-membrane-type matrix metalloproteinase-1 (MT1-MMP, MMP-14), lacking the transmembrane and cytoplasmic domains, was expressed in *E. coli* (*36*). During in vitro folding, the zymogen underwent autocatalytic activation to produce a truncated active form [MT1-MMP(ΔC)] as previously described (*36*).

ProMMP-1(E200A), a catalytically inactive mutant of MMP-1, was expressed in *E. coli* and folded from inclusion bodies as for the wild-type enzyme (*31*). Purified proMMP-1(E200A) was activated using MMP-3(ΔC) and APMA as described for wild-type proMMP-1. MMP-1(E200A) affinity resin was prepared by coupling 2 mg of MMP-1(E200A) to N-hydroxysuccinimide-activated HiTrap Sepharose (1 mL, Amersham BioSciences, Uppsala, Sweden) according to the manufacturer's instructions.

Human recombinant TIMP-1 was expressed in CHO-K-1 cells and purified from the conditioned medium (*37*). Human recombinant TIMP-2 was expressed using the mammalian expression vector pCEP4 (Invitrogen, Carlsbad, CA), transfected into 293-EBNA cells (Invitrogen, Carlsbad, CA) using FuGENE6™ (Roche Molecular Biochemicals, Indianapolis, IN) according to the manufacturer's instructions. TIMP-2 was purified from conditioned medium using Green A Dyematrex (Millipore, Bedford, MA) and gel filtration with S-200 (Amersham BioSciences, Uppsala, Sweden) (*38*).

α_2-Macroglobulin (α_2M) was a gift from Professor Lars Sottrup-Jensen, University of Aarhus, Aarhus, Denmark. The hydroxamate inhibitor GM6001-X [$HONHCOCH_2CH$-(isobutyl) CO-Tyr(OMe)-NHMec (*39*)] was a gift from Dr J. Oloksyszyn of OsteoArthritis Sciences, Inc. (Cambridge, MA).

Construction of TIMP-4/pET3a. Human TIMP-4 cDNA was isolated as previously described (*17*). Full-length human TIMP-4 was amplified by polymerase chain reaction from TIMP-4-containing cDNA using the sense primer 5′-GAA GGA GAT ATA CAT ATG TGC AGC TGC GCC CCG GCG CAC CC-3′ and the anti-sense primer 5′-TTG TTA GCA GCC GGA TCC CTA GGG CTG AAG GAT GTC AAC AA-3′ (*Nde*I and *BamH*1 sites in the sense and antisense primer respectively underlined). The product was digested with *BamH*1 and *Nde*I (New England BioLabs, Beverly, MA) and ligated into similarly cut pET3a expression vector (Novagen, Madison, WI) using T4 DNA ligase (Invitrogen, Carlsbad, CA). The sequence of the final ligation product was confirmed using the T7 promoter primer by automated DNA sequencing at the Biotech Facility of the University of Kansas, KS.

Expression and Refolding of Recombinant TIMP-4. Competent *E. coli* BL21 (DE3) were transformed with TIMP-4/pET3a and grown in Luria Bertani Broth with 50 μg/mL carbenicillin. Expression was induced by addition of 0.4 mM isopropylthio-β-galactosidase (Fisher Scientific, Springfield, NJ) for 3 h at 37 °C and inclusion bodies prepared by treatment of cells with lysozyme, deoxycholate, and DNAse I. Inclusion bodies were solubilized in 8 M urea, 50 mM Tris/HCl, pH 8.0, 20 mM dithiothreitol, and insoluble material was removed by centrifugation (15 min, 10 000*g*). Acetic acid was added to alter the pH of the supernatant to pH 5.5 and the material applied onto a MacroPrep S cation-exchange resin (2.5 × 5 cm, BioRad, Hercules, CA) equilibrated in 8 M urea, 50 mM sodium acetate, pH 5.5, 1 mM dithiothreitol. The column was washed with equilibration buffer, and TIMP-4-containing fractions were eluted in 8 M urea, 50 mM Tris/HCl, pH 8.6, 50 mM NaCl, 1 mM dithiothreitol and identified by SDS-PAGE (*40*). TIMP-4-containing fractions were applied to a MacroPrep Q anion-exchange resin (2.5 × 5 cm, BioRad, Hercules, CA) equilibrated in 8 M urea, 50 mM Tris/HCl, pH 8.6, 50 mM NaCl, 1 mM dithiothreitol. TIMP-4 eluted in the unbound fraction, while contaminants, including DNA, adhered to the resin. Purified TIMP-4 was folded essentially according to the TIMP-2-folding method described by Wingfield et al. (*41*). Cystamine (20 mM) was added to the TIMP-4-containing fractions and the solution stirred overnight to allow the formation of mixed disulfides. This material was then introduced dropwise into a 10-fold volume of 100 mM Tris/HCl, pH 8.0, 2.5 M urea, 5 mM reduced glutathione, 1 mM oxidized glutathione, 1 mM Na_2EDTA, 0.02% NaN_3 (~8 h, 4 °C). The sample was then sequentially dialyzed against 5 and 15 volumes of 50 mM Tris/HCl, pH 8.0, 0.02% NaN_3 (10−12 h each) and concentrated to ~20 mL on an Amicon YM-10 membrane (Millipore, Bedford, MA). Misfolded forms had lower solubility and precipitated upon concentration. TIMP-4 was applied to MMP-1(E200A)-Sepharose equilibrated in 50 mM Tris/HCl, pH 7.5, 0.15 M NaCl, 5 mM $CaCl_2$, 50 μM $ZnCl_2$, 0.02% NaN_3. Bound material was eluted with 0.1 M glycine, pH 2.7, 0.02% NaN_3, directly into 1/10 final fraction volume of 1 M Tris/HCl, pH 8.0, to ensure rapid neutralization of the eluate. Pooled

TIMP-4 fractions were dialyzed twice (10−12 h, 4 °C) against 10 volumes of 50 mM Tris/HCl, pH 7.5, 0.15 M NaCl, 5 mM $CaCl_2$, 50 μM $ZnCl_2$, 0.02% NaN_3.

Fluorometric Enzyme Assays. Enzyme assays were performed using the synthetic substrate Mca-Pro-Leu-Gly∼Dpa-Ala-Arg-NH_2 (1.5 μM, Bachem, Bubendorf, Switzerland), where ∼ indicates the scissile bond and Mca and Dpa are (7-methoxycoumarin-4-yl)acetyl and 3-(2,4-dinitrophenyl)-L-2,3-diaminopropionyl, respectively (*42*). Assays were conducted at either 25 or 37 °C in TNC buffer (50 mM Tris/HCl, pH 7.5, 0.15 M NaCl, 10 mM $CaCl_2$, 0.02% NaN_3, 0.05% Brij 35). Fluorescence was monitored using a Perkin-Elmer (Beaconsfield, U.K.) LS-50B luminescence spectrometer with an excitation wavelength of 325 nm and an emission wavelength of 393 nm. Total substrate hydrolysis was less than 5% in all cases. Active MMP concentrations were determined by titrating the enzymes (5−200 nM) against TIMP-1 (50 nM) of known concentration.

MALDI Mass Spectrometry of Trypsin-Digested TIMP-4. The MMP-1 (E200A)-Sepharose resin separated the folded TIMP-4 into two pools: a fully active bound fraction and an inactive unbound fraction. To further characterize these two species, we performed matrix-assisted laser desorption ionization (MALDI) mass spectrometry on trypic digests of the active and inactive TIMP-4. Reduction, carbamidomethylation of cysteines, and in-gel digestion with trypsin were performed according to published methods (*43*−*45*) modified for use with a robotic digestion system (*46*) (Investigator ProGest, Genomic Solutions, Huntington, U.K.). MALDI mass spectra were recorded with a TofSpec 2E spectrometer (Micromass, Manchester, U.K.), equipped with a 337 nm nitrogen laser and operated in the positive ion reflectron mode at 20 kV accelerating voltage. The matrix was a mixture of α-cyano-4-hydroxy-cinnamic acid and nitrocellulose, applied to the target as a microcrystalline thin film by a modification of the procedure of Vorm et al (*47*). Spectra were internally calibrated using trypsin autolysis products, and the resulting peptide mass fingerprints were searched against a local copy of SwissProt/TREMBL using ProteinLynx Global Server (Version 1, Micromass, Manchester, U.K.). One missed cleavage per peptide was allowed, and an initial mass tolerance of 100 ppm was used in all searches. Cysteines were assumed to be carbamidomethylated, but other potential modifications were not considered in the first pass search.

HPLC and ESI MS/MS of Active and Inactive TIMP-4. ESI MS/MS (electrospray ionization tandem mass spectrometry) spectra were recorded using a Q-Tof hybrid quadrupole/orthogonal acceleration time-of-flight spectrometer (Micromass, Manchester, U.K.) interfaced to a Micromass CapLC capillary chromatograph. Samples were dissolved in aqueous formic acid, and aliquots were injected onto a desalting column of Pepmap C18 (LC Packings, Amsterdam), washed with 0.1% aqueous formic acid, then eluted into the mass spectrometer with an acetonitrile/0.1% formic acid gradient. The capillary voltage was set to 3500 V, and data-dependent MS/MS acquisitions were performed on precursors with charge states of 2, 3, or 4 over a survey mass range 540−1000. The collision gas was argon, and the collision voltage was varied between 18 and 45 V, depending on the charge-state and mass of the precursor. Proteins were identified by correlation of uninterpreted tandem mass spectra to entries in SwissProt/TREMBL using ProteinLynx Global Server.

Progress Curves to Determine k_{on} and K_i. All kinetic parameters were determined for TIMP-1 as well as for TIMP-4 to allow comparison of the values determined in the present study with previously published data for TIMP-1. K_i and k_{on} were determined from the equilibrium and preequilibrium phases of progress curves respectively (*48*, *49*).

The rate of MMP-TIMP association was monitored by addition of MMP (0.1−5 nM) to a mixture of TIMP ($[I]_o$ = 1−100 nM) and 1.5 μM substrate, preequilibrated to 25 °C for MT1-MMP and MMP-2 and to 37 °C for all other tested enzymes. In all cases, $[I]_o > 10[E]_o$ and substrate hydrolysis was less than 5%. Since $[S]_o < K_m$, it was not necessary to include terms to compensate for substrate competition (*48*). For MMP-1, MMP-1(ΔC), MMP-3, and MMP-3(ΔC), 5 nM enzyme was used, with 50−100 nM TIMP-1 or TIMP-4. For MMP-2 and MT1-MMP, 0.1 nM enzyme was used, with 1−5 nM TIMP for MMP-2 and 3−12 nM TIMP-4 for MT1-MMP. At least five concentrations of inhibitor were analyzed. The biphasic progress curves were followed until equilibrium was reached (about 1.5−2 h), and data were fitted to the integrated rate equation:

$$\Delta F = v_s t + (v_o - v_s)(1 - e^{-kt})/k \quad (1)$$

where ΔF is the increase in product fluorescence, v_o and v_s are the initial and steady-state reaction velocities, respectively, t is time, and k is the pseudo-first-order rate constant for the establishment of equilibrium between enzyme and inhibitor (*50*). Data were analyzed using the program EnzFitter (BioSoft, Cambridge, U.K.). Linear regression analysis of the dependence of k on TIMP concentration indicated that inhibition over the concentration range studied was adequately described by a simple bimolecular model, allowing calculation of k_{on}, the second order or association rate constant from the gradient of the plot (*51*).

Since substrate concentrations were well below K_m, the same progress curves could be used to calculate K_i (the equilibrium dissociation constant), using the equation

$$[I]_o/(1 - a) = K_i/a + [E]_o \quad (2)$$

where [I] is the TIMP concentration and $a = v_s/v_o$ (*48*). A plot of $1/a$ versus $[I]_o/(1 - a)$ gave a straight line with a gradient equal to K_i and a Y-intercept of $[E]_o$. The dissociation rate constant, k_{off}, was calculated from the relationship $K_i = k_{off}/k_{on}$ (*48*).

Direct Calculation of k_{off} Using α_2M. While the above methodology allows for indirect determination of k_{off} from the progress curve, we sought to confirm our low K_i values for TIMP-4 by direct determination of k_{off} using the proteinase inhibitor α_2M to irreversibly trap enzyme dissociating from MMP-TIMP complexes. While proteinases bound to α_2M are inactive against protein substrates, small synthetic substrates are able to gain access to α_2M-trapped proteinases and are readily hydrolyzed. As more MMP dissociates from TIMP and becomes trapped by α_2M, substrate hydrolysis increases exponentially and can be used as a measure of complex dissociation (*52*). MMP (100 nM) was preincubated with TIMP (100 nM) for 1 h at 37 °C to form a 1:1 enzyme/inhibitor complex. The MMP−TIMP complex (diluted to 5

nM) was incubated with α_2M (50−400 nM) and synthetic substrate (1.5 μM, 200 μL reaction volume). Fluorescence was measured every 10 min for up to 4 h using a Molecular Devices (Sunnyvale, CA) microplate fluorimeter. All assays were carried out in triplicate.

To calculate k_{off}, the concentration of inhibited enzyme at each time point, [EI], was determined and expressed as a fraction of initial enzyme/inhibitor complex concentration, $[EI]_o$ (=5 nM). Since $[EI] = [EI]_o - [\alpha_2M-enzyme]$, a standard curve was drawn up to convert fluorescence measured every 10 min to $[\alpha_2M-enzyme]$. The standard curve was constructed by incubating each MMP (25 nM) with α_2M (125 nM, 1 h, 37 °C) and assaying dilutions of this α_2M-treated MMP in 10 min stopped-time assays.

Once $[EI]/[EI]_o$ was known for each time point, k_{off} was calculated by linear regression of $\ln [EI]/[EI]_o$ on t, using the equation (*52*)

$$\ln \frac{[EI]}{[EI]_o} = -k_{off}t \quad (3)$$

Effect of pH on Inhibition. We investigated the effect of pH on TIMP-1, -2, and -4 inhibition of MMP-1(Δ*C*) and MMP-3(Δ*C*) by determining K_i and k_{on} from progress curves at various pHs. Progress curves were measured as described above, except that TNC assay buffer was replaced by AMT buffer (50 mM acetate, 50 mM Mes, 50 mM Tris/HCl, 5 mM $CaCl_2$, 0.05% Brij 35, 0.02% NaN_3). This buffer system, which is effective from pH 4.0−9.0, ensures that a constant ionic strength is maintained across the pH range studied (*53*).

Analysis of TIMP-MMP Molecular Interactions Using IAsys Resonance Mirror Biosensor. The interactions of TIMPs with various MMPs (and their constituent domains) were analyzed using an IAsys resonance mirror biosensor. This technique, similar to Biacore analysis, detects binding of a test protein to an immobilized ligand as changes in the refrective index of the solution immediately adjacent to a resonance mirror sensor surface. Using an IAsys Plus biomolecular analysis system (Affinity Sensors, Cambridge, U.K.), TIMP-1, TIMP-2, and TIMP-4 (1.5 μg each) were covalently coupled to carboxymethyl dextran sensor chips (Affinity Sensors, Cambridge, U.K.) via free amino groups using N-hydroxysuccinimide/1-ethyl-3-(3-dimethylaminopropyl) carbodiimide coupling chemistry. Bovine serum albumin (1.5 μg) was coupled as a negative control for each TIMP. Remaining activated sites on the sensor surface were blocked with 1 M Tris/HCl, pH 8.0. Between 750 and 1000 arc seconds of TIMP or BSA were coupled, corresponding to between 5 and 20 ng of protein per well. MMP ligands under study were applied to the sensor surface in TNC buffer (concentrations ranging from 10 to 500 nM, 25 °C). To test the relative contributions of MMP N- and C-terminal domains to the overall interaction, the MMP under study was in some cases preincubated with the active site-blocking hydroxamate GM6001-X (10 μM, 30 min, 37 °C) (*54*) and reacted with TIMPs in the presence of 10 μM GM6001-X. Chips were regenerated with a 15 s application of 50 mM HCl. Control binding experiments were performed at various stages in the analysis to confirm that the regeneration conditions had not altered the binding capacity of the coupled TIMP. k_{off} was too slow to be directly observed over the time course of the experiment (~30 min). The association phase, however, was clearly observed and fitted to the following equation using FastFit software (Affinity Sensors, Cambridge, U.K.):

$$R_t = R_0 + R_{max}(1 - e^{-k_{obs}t}) \quad (4)$$

where R_t is the sensor response (in arc seconds) at time, t, R_0 is the response at time = 0, R_{max} is the maximum response at infinite time, and k_{obs} is the observed association rate constant. Linear regression of k_{obs} on MMP concentration provided k_{on} and k_{off} from the gradient and Y-intercept, respectively. K_D was calculated as k_{off}/k_{on}.

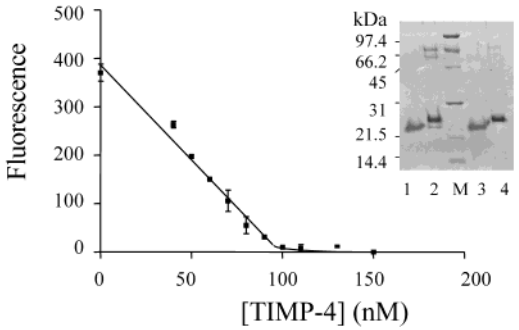

FIGURE 1: Titration of TIMP-4 with MMP-3(ΔC). TIMP-4 (40−150 nM) was incubated with MMP-3(ΔC) (100 nM) at 37 °C for 1 h, and residual activity against Mca-Pro-Leu-Gly~Dpa-Ala-Arg-NH_2 (1.5 μM) was determined. Inset, SDS-PAGE (12% acrylamide) analysis of inactive TIMP-4 (1.2 μg, lane 1, without reduction; lane 2, with reduction) and active TIMP-4 (1.2 μg, lane 3, without reduction; lane 4, with reduction). Proteins were stained with Coomassie Blue. M, molecular mass markers.

RESULTS

TIMP-4 Expression and Folding. This study provides the first description of expression and in vitro folding of recombinant human TIMP-4 from *E. coli*. Following two ion exchange steps to remove contaminating material, TIMP-4 was folded by slow dilution into a buffer containing a 5:1 molar ratio of reduced:oxidized glutathione. Approximately 1 mg of folded TIMP-4 was obtained and the preparation was 95% pure based on SDS-PAGE analysis. However, only 7% of the inhibitor was active when titrated with MMP-3(ΔC). To separate active and inactive TIMP-4, the sample was applied to a MMP-1(E200A)-Sepharose affinity resin. Inactive TIMP-4 passed through the column, while active TIMP-4 bound to the column and was eluted with an acid wash. A yield of 50 μg of TIMP-4 per L of bacterial expression was obtained. The 1:1 stoichiometry of inhibitory activity against MMP-3(ΔC) indicated that the TIMP-4 fraction binding to the resin was 100% active (Figure 1). SDS-PAGE analysis showed a single band of 23 kDa under reducing conditions, in accordance with a mass of 22.3 kDa predicted from the primary structure (*17*) (Figure 1, inset). Samples run under non-reducing conditions exhibited a slightly increased mobility, indicating that disulfide bond formation had occurred during folding. Inactive TIMP-4, which did not bind to the MMP-1(E200A) resin, exhibited a similar shift in apparent molecular mass upon reduction, indicating that was also correctly folded (Figure 1, inset).

MALDI and Electrospray Mass Spectrometry. Active (bound) and inactive (unbound) TIMP-4 fractions from MMP-1(E200A)-Sepharose were further characterized by

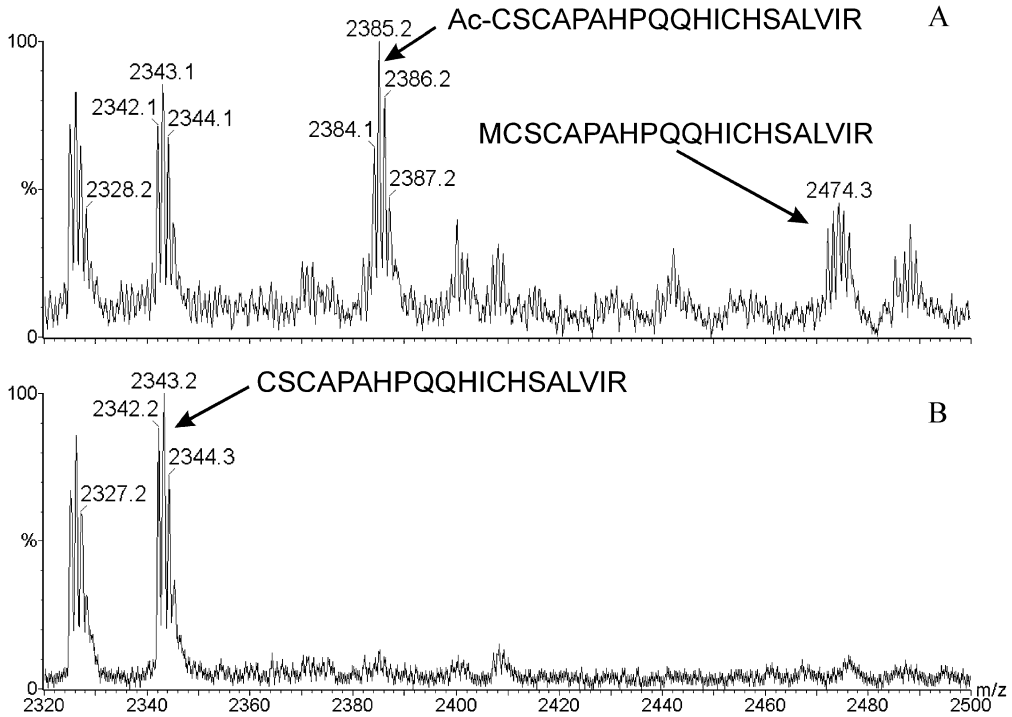

FIGURE 2: MALDI mass spectrometry of inactive and active TIMP-4. Inactive and active TIMP-4 bands were excised from SDS-PAGE gels and digested with trypsin. The resulting peptides were subjected to MALDI mass spectrometry. For inactive TIMP-4 (A), peptides corresponding in mass to wild-type TIMP-4 (CSCAPAHPQQHICHSALIVIR) as well as N-terminally acetylated TIMP-4 (Ac−CSCAPAHPQQHICHSALIVIR) and Met-TIMP-4 (MCSCAPAHPQQHICHSALIVIR) were detected. For active TIMP-4 **(B)**, only the wild-type form of this N-terminal peptide was present (CSCAPAHPQQHICHSALIVIR).

mass spectrometry. Following in-gel trypsin digestion of the active and inactive TIMP-4 samples, peptides were analyzed by both MALDI and electrospray mass spectrometry. MALDI analysis of active TIMP-4 identified a peptide corresponding in mass to the N-terminal peptide predicted to result from trypsin digestion of wild-type TIMP-4 (CSCAPAHPQQHICHSALIVIR, Figure 2B). Generation of de novo sequence data by electrospray mass spectrometry confirmed the sequence of this N-terminal peptide. MALDI analysis of the inactive TIMP-4 identified two additional peptides whose molecular masses are consistent with N-terminal acetylation of TIMP-4 and the presence of an additional methionine at the N-terminus of the protein (Ac−CSCAPAHPQQHICHSALIVIR and MCSCAPAHPQQHICHSALIVIR, Figure 2A).

Determination of k_{on} and K_i with MMPs. Kinetic parameters were determined for four prototype MMPs, MMP-1 (collagenase 1), MMP-2 (gelatinase A), MMP-3 (stromelysin 1), and MMP-14 (MT1-MMP). Biphasic progress curves were observed, typical of reversible, tight-binding inhibition (*48*). A typical progress curve is shown in Figure 3, for the inhibition of MT1-MMP(ΔC) by TIMP-4. Progress curves were fitted to the integrated rate equation (eq 1) to determine *k*, the pseudo-first-order rate constant, for each TIMP concentration. In all cases, there was a good fit between the experimental data points and the theoretical curve generated using eq 1. Linear regression of *k* on TIMP concentration indicated that a simple bimolecular model adequately described the data and k_{on} was calculated from the gradient of a plot of TIMP concentration versus *k*. In accordance with previously published data for MMP inhibition by TIMPs, k_{on} values were on the order of 10^5 M^{-1} s^{-1} (Table 1). K_i values, calculated using steady-state velocities from the equilibrium part of the progress curves, were in the low nanomolar range, except in the case of MMP-2, where K_i was in the picomolar range (Table 1).

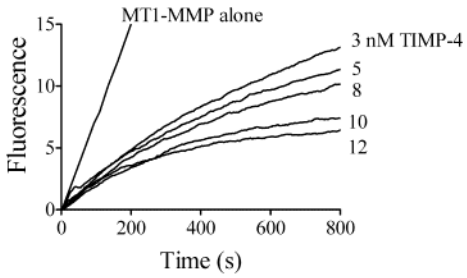

FIGURE 3: Progress curves showing TIMP-4 inhibition of MT1-MMP(ΔC). TIMP-4 (3−12 nM) was added to a solution of MT1-MMP(ΔC) (0.1 nM) and Mca-Pro-Leu-Gly∼Dpa-Ala-Arg-NH_2 (1.5 μM) preequilibrated to 25 °C, and product fluorescence was monitored. Data were fitted to eq 1 to determine *k*, the pseudo-first-order rate constant for each TIMP-4 concentration.

Direct Determination of k_{off} Using α_2M. To determine the k_{off} rate of TIMP-MMP complexes, we employed some of the unique properties of α_2M, namely, (i) only proteolytically active endopeptidases form an irreversible complex with α_2M; (ii) reactions of MMPs with α_2M are rapid, especially in a large excess of α_2M (*55*), and (iii) the enzymatic activity of α_2M-bound MMPs can be detected using a sensitive synthetic substrate. Thus, this system allowed us to measure the amount of enzyme dissociating from the TIMP-MMP complex from the exponential increase in substrate hydrolysis over time. Experiments carried out at different α_2M concentrations (50, 100, 200, 300, and 400 nM) confirmed that k_{off} is independent of α_2M concentration under the conditions used (>10-fold excess of α_2M over TIMP−MMP complex). A typical exponential increase in the rate of substrate

Table 1: K_i and k_{on} Values for TIMP-4 and TIMP-1 Inhibition of MMPs[a]

	TIMP-4		TIMP-1	
	k_{on} ($\times 10^{-5}$ M^{-1} s^{-1})	K_i (nM)	k_{on} ($\times 10^{-5}$ M^{-1} s^{-1})	K_i (nM)
MMP-1	2.03 ± 0. 19	0.65 ± 0.10	1.59 ± 0.14	0.38 ± 0.02
MMP-1(ΔC)	1.13 ± 0.17	2.59 ± 0.23	0.52 ± 0.07	2.11 ± 0.41
MMP-2 (25 °C)	45.9 ± 10.0	0.004 ± 0.001	26.21 ± 6.40	0.014 ± 0.001
MMP-3	0.71 ± 0.12	1.51 ± 0.21	2.00 ± 0.24	0.63 ± 0.10
MMP-3(ΔC)	0.49 ± 0.07	1.24 ± 0.11	1.20 ± 0.20	1.08 ± 0.18
MT1-MMP(ΔC) (25 °C)	2.29 ± 0. 71	0.73 ± 0.09	ND	ND

[a] TIMP-1 and TIMP-4 ($[I]_o$ = 5−100 nM) inhibition of MMPs (0.1−5 nM) was assessed using progress curve analysis at 37 °C unless otherwise stated. Data were fitted to eqs 1 and 2 to determine k_{on} and K_i respectively. Errors shown are standard errors of the mean. ND: Not determined

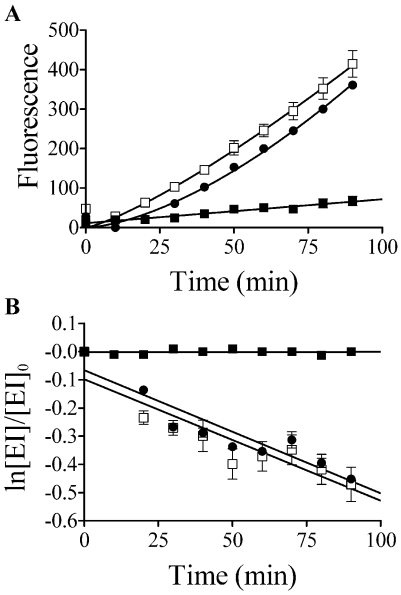

FIGURE 4: Calculation of k_{off} for TIMP-4/MMP-1 dissociation using α_2M. (A) MMP-1 (100 nM) and TIMP-4 (100 nM) were preincubated to form a 1:1 equilibrium complex. The equilibrium complex was diluted to 5 nM with α_2M (300 or 400 nM) and 1.5 μM Mca-Pro-Leu-Gly∼Dpa-Ala-Arg-NH_2 (200 μL reaction volume), and fluorescence measured every 10 min. Samples incubated with α_2M showed higher activity than those incubated without α_2M (■). Data obtained with 300 nM (●) and 400 nM (□) α_2M are shown. Error bars represent standard deviations of the mean from triplicate runs. (B) Using a standard curve constructed with α_2M-treated MMP-1, fluorescence measured at each time point was converted to a concentration of α_2M−enzyme. Since [EI] = $[EI]_o$ − [α_2M−enzyme], the fraction of inhibited enzyme ($[EI]/[EI]_o$) could be calculated and k_{off} calculated as the gradient of a plot of ln [EI]/$[EI]_o$ vs time.

hydrolysis is shown in Figure 4A. Using this method, we calculated a k_{off} value for TIMP-4 dissociation from MMP-1 of 8.07 (± 0.05) × 10^{-5} s^{-1} (Figure 4B). Dividing this by the k_{on} value calculated from the progress curve (Table 1, 2.03 × 10^5 M^{-1} s^{-1}) gives a K_i value of 0.4 nM, which compares well with the value of 0.65 nM determined from the equilibrium part of the progress curve. Similarly, using α_2M, we determined a k_{off} value for TIMP-4 dissociation from MMP-3 of 7.61 (± 0.16) × 10^{-5} s^{-1}. Dividing this by the k_{on} value calculated from the progress curve (Table 1, 0.71 × 10^5 M^{-1} s^{-1}) gives a K_i value of 1.07 nM, comparing well with the value of 1.51 nM determined from the equilibrium part of the progress curve. For MMP-2, dissociation was too slow to be observed over the time course of the experiment (∼2 h). Once trapped by α_2M, MMPs are generally still able to hydrolyze small synthetic substrates,

Table 2: pH Dependence of K_i for TIMP Inhibition of MMP-1(ΔC) and MMP-3(ΔC)[a]

	K_i (nM)			
	TIMP-1	TIMP-2	TIMP-4	
pH	MMP-3(ΔC)	MMP-3(ΔC)	MMP-1(ΔC)	MMP-3(ΔC)
9.0	ND	ND	0.36 ± 0.06	1.21 ± 0.54
8.5	0.72 ± 0.18	0.64 ± 0.06	0.20 ± 0.06	1.04 ± 0.85
8.0	0.19 ± 0.02	0.81 ± 0.23	0.21 ± 0.06	0.85± 0.23
7.5	0.15 ± 0.01	1.03 ± 0.16	0.33 ± 0.04	0.51 ± 0.22
7.0	1.20 ± 0.48	1.41 ± 0.15	0.68 ± 0.02	0.24 ± 0.04
6.5	2.29 ± 0.08	1.30 ± 0.22	0.74 ± 0.02	0.20 ± 0.06
6.0	2.50 ± 0.33	4.80 ± 1.09	0.86 ± 0.02	0.46 ± 0.02
5.5	9.97 ± 1.3	13.52 ± 1.43	1.12 ± 0.39	2.49 ± 0.56
5.0	10.46 ± 1.5	ND	7.38 ± 0.81	5.42 ± 1.14
4.5	ND	ND	ND	6.54 ± 1.72

[a] K_i values for TIMP-1, TIMP-2, and TIMP-4 ($[I]_o$ = 10−250 nM) inhibition of MMP-1(ΔC) and MMP-3(ΔC) (1 nM) were measured as described for Table 1, except that pH was varied between pH 4.5 and 9.0 using a constant ionic strength AMT buffer (50 mM acetate, 50 mM Mes, 50 mM Tris/HCl). Errors shown are standard errors of the mean. ND: Not able to be determined.

but their catalytic rates with these substrates may be altered. α_2M-bound MMP-3 was slightly less active against the synthetic substrate than the free enzyme, while α_2M-bound MMP-1 hydrolyzed the substrate more rapidly. Interestingly, α_2M-bound MT1-MMP was essentially inactive (less than 5%) against the synthetic substrate, preventing calculation of a k_{off} value using this method (results not shown).

Effect of pH on TIMP Inhibition. The crystal structures of TIMP-MMP complexes (*2*, *27*) suggest that the N-terminal α-amino group of TIMP needs to be deprotonated to interact with the catalytic Zn^{2+} of an MMP. Since pH will affect the charge on this N-terminal α-amino group, we predicted that TIMP inhibition of MMPs would be pH-dependent. Progress curve analysis showed this is indeed the case, with K_i increasing (Table 2) and k_{on} decreasing (Figure 5) with decreasing pH for TIMP-1, TIMP-2, and TIMP-4 inhibition of MMP-1(ΔC) and MMP-3(ΔC). At extreme pH values (pH >8.5 and pH <5.0), MMP activity was substantially reduced, making reliable determination of K_i difficult. It was, however, still possible to accurately determine k_{on} at these pH values, as shown in Figure 5.

The pH profile of inhibition by TIMPs was confirmed to be independent of the pH profile of enzymatic activity (data not shown) as expected, since k_{on} is a function of the ratio between inhibited and uninhibited activity at each pH. K_i and k_{on} were lower and higher, respectively, when determined in AMT buffers compared to TNC buffers [compare MMP-3(ΔC) values in Table 1 and Figure 5]. This indicates that

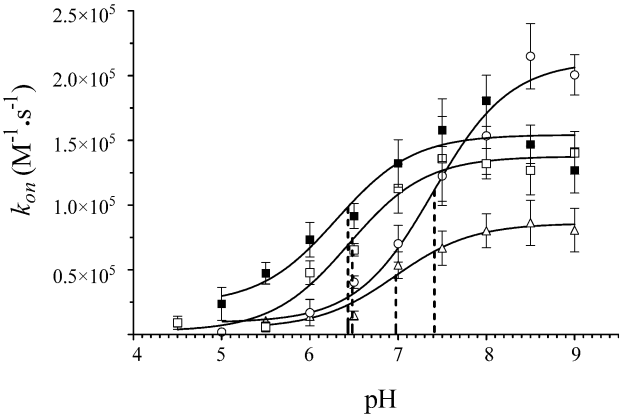

FIGURE 5: Effect of pH on TIMP-1, TIMP-2, and TIMP-4 inhibition of MMP-1(ΔC) and MMP-3(ΔC). k_{on} was determined from pre-steady-state progress curves, in constant ionic strength 50 mM acetate, 50 mM Mes, 50 mM Tris/HCl, 5 mM $CaCl_2$, 0.05% Brij 35, 0.02% NaN_3 (AMT) buffers. For TIMP-4 inhibition of MMP-1(ΔC) (■) and MMP-3(ΔC) (□), half-maximal k_{on} values were observed at pH 6.4. For TIMP-1 (○) and TIMP-2 (△) inhibition of MMP-3(ΔC), half-maximal k_{on} values were observed at pH 7.4 and pH 7.0, respectively.

Table 3: IAsys Biosensor Analysis of Binding between immobilized TIMP-1 and Various MMP Ligands

MMP	k_{on} ($\times 10^{-5}$ M^{-1} s^{-1})	k_{off} (s^{-1})	K_D (nM)
ProMMP-1	no binding		
MMP-1	0.379	0.0009	23
MMP-1 + GM6001-X	no binding		
MMP-1(ΔC)	0.043	0.0010	247
MMP-1(ΔC) + GM6001-X	no binding		
ProMMP-2	no binding		
MMP-2	0.379	0.0014	39
MMP2 + GM6001-X	no binding		
HPX_{MMP-2}	no binding		
ProMMP-3	no binding		
MMP-3	0.108	0.0002	24
MMP3 + GM6001-X	no binding		
MMP-3(ΔC)	0.057	0.0005	95
MMP-3(ΔC) + GM6001-X	no binding		
MT1-MMP(ΔC)	no binding		

ionic strength affects inhibition constants and reiterates the importance of using constant ionic strength AMT buffers for this study.

In all cases studied, k_{on} decreased with decreasing pH below pH 8.0 (Figure 5). The variation of k_{on} with pH was similar for TIMP-4 inhibition of MMP-1(ΔC) and MMP-3(ΔC), and differed from the pH profile for TIMP-1 and TIMP-2 inhibition of MMP-3(ΔC) (Figure 5). For TIMP-4, half-maximal k_{on} values were at pH 6.4, while for TIMP-1 and TIMP-2, half-maximal k_{on} values were at pH 7.4 and 7.0, respectively. K_i values for TIMP-4 inhibition of MMP-1(ΔC) and MMP-3(ΔC) were relatively constant above pH 6.0 and increased below pH 5.5 (Table 2). In comparison, K_i values for TIMP-1 and TIMP-2 inhibition of MMP-3(ΔC) were constant above pH 6.5 and increased below pH 6.0. Thus, TIMP-4 retained higher reactivity with MMPs in an acidic environment than either TIMP-1 or TIMP-2.

Analysis of Mode of Interaction between TIMP and MMP. The interactions of TIMP-4 with various MMPs were measured by IAsys biosensor analysis and compared with those of TIMP-1 and TIMP-2 (Tables 3 to 5). For data analysis we used a simple monophasic binding model

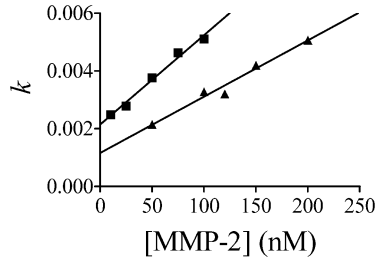

FIGURE 6: IAsys analysis of TIMP-4 and TIMP-2 interaction with MMP-2. Various concentrations of MMP-2 (10−200 nM) were added to immobilized TIMP-4 (■) and TIMP-2 (▲). Association was analyzed using FastFit software (Affinity Sensors, Cambridge, U.K.). There was a linear correlation between k and MMP concentration, indicating that a simple monophasic binding model adequately described the data. Values for k_{on} and k_{off} were calculated from the gradient and Y-intercept, respectively, and K_D was calculated as k_{off}/k_{on}.

because it gave a linear correlation between MMP concentration and k (Figure 6), and the error was less than 1% in all cases. K_D values determined are summarized in Tables 3 to 5. On average, K_D values were 2 orders of magnitude higher than K_i values. This is likely to be due to the influence of factors such as constraint of one of the interacting partners on the sensor surface, chemical modification concomitant with immobilization and variation in the orientation of the immobilized molecule (*56*). Despite this limitation, the analysis enabled us to dissect the relative contributions of each domain to the overall molecular interaction (e.g., proMMP-2, hydroxamate-inhibited MMPs and HPX_{MMP-2}).

As expected, none of the tested TIMPs bound to proMMP-1 or proMMP-3, and they failed to bind to active MMP-1 and MMP-3 in the presence of the low molecular weight active site-directed hydroxamate inhibitor GM6001-X (Table 3). In most cases, the binding affinities of TIMPs for MMP-1(ΔC) and MMP-3(ΔC) were weaker than those for the full-length enzymes. On the basis of the IASys analysis, the C-terminal HPX domains of these MMPs make a contribution to the overall free energy of binding, although they alone are unable to support binding. MMP-3 is inhibited more strongly by TIMP-1 than by TIMP-2 or TIMP-4.

Both TIMP-2 and TIMP-4, but not TIMP-1, bound to proMMP-2 and the isolated C-terminal HPX_{MMP-2} (Tables 3 to 5) as reported previously (*10*, *51*, *57*). However, the K_D values of TIMP-2 for proMMP-2 and for full-length active MMP-2 were essentially identical. It is striking that, unlike other MMPs, the binding of TIMP-2 to MMP-2 was not blocked nor was the affinity altered in the presence of the hydroxamate inhibitor GM6001-X, even at a very high concentration (50 μM). Given that the K_i of GM6001-X for MMP-2 inhibition was 0.7 nM (results not shown), this concentration of GM6001-X should completely block the MMP-2 active site. We therefore concluded that when the active site of MMP-2 is blocked by GM6001-X, TIMP-2 binds to MMP-2 through the HPX_{MMP-2}, as in the case of proMMP-2 (see Figure 7). The K_D of TIMP-2 for HPX_{MMP-2} alone was slightly higher than for proMMP-2 or GM6001-X-inhibited MMP-2, suggesting that there is an additional minor interaction formed with the full-length MMP-2 or proMMP-2.

TIMP-4, on the other hand, exhibited different binding parameters (Table 5). The affinity of TIMP-4 for proMMP-2 was about 5-fold lower than that for the active MMP-2. In

Table 4: IAsys Biosensor Analysis of Binding between Immobilized TIMP-2 and Various MMP Ligands

MMP	[GM6001-X] (μM)	k_{on} ($\times 10^{-5}$ M^{-1} s^{-1})	k_{off} (s^{-1})	K_D (nM)
ProMMP-1	−	no binding		
MMP-1	−	0.362	0.0014	39
MMP-1 + GM6001-X	10.00	no binding		
MMP-1(ΔC)	−	0.385	0.0026	69
MMP-1(ΔC) + GM6001-X	10.00	no binding		
ProMMP-2	−	0.225	0.0016	71
ProMMP-2 + GM6001-X	10.00	0.243	0.0017	70
MMP-2	−	0.195	0.0011	60
MMP-2 + GM6001-X	10.00	0.267	0.0016	60
	50.00	0.263	0.0015	57
HPX_{MMP-2}	−	0.051	0.0006	117
HPX_{MMP-2} + GM6001-X	10.00	0.050	0.0005	107
ProMMP-3	−	No binding		
MMP-3	−	0.018	0.0013	706
MMP-3 + GM6001-X	10.00	No binding		
MMP-3(Δ*C*)	−	0.015	0.0016	1020
MMP-3(ΔC) + GM6001-X	10.00	No binding		
MT1-MMP(Δ*C*)	−	0.154	0.0041	269
MT1-MMP(ΔC) + GM6001-X	10.00	No binding		

Table 5: IAsys Biosensor Analysis of Binding between Immobilized TIMP-4 and Various MMP Ligands

MMP	[GM6001-X] (μM)	k_{on} ($\times 10^{-5}$ M^{-1} s^{-1})	k_{off} (s^{-1})	K_D (nM)
ProMMP-1	−	no binding		
MMP-1	−	1.18	0.0068	58
MMP-1 + GM6001-X	10.00	no binding		
MMP-1(ΔC) −	0.079	0.0025	319	
MMP-1(ΔC) + GM6001-X	10.00	no binding		
ProMMP-2	−	0.066	0.0022	333
ProMMP-2 + GM6001-X	10.00	0.083	0.0028	345
MMP-2	−	0.309	0.0021	70
MMP-2 + GM6001-X	0.001	0.260	0.0017	65
	0.010	0.240	0.0019	79
	0.015	0.230	0.0023	100
	0.020	0.205	0.0022	107
	0.025	0.182	0.0024	132
	0.050	0.142	0.0026	183
	10.000	0.084	0.0029	345
HPX_{MMP-2}	−	0.036	0.0013	380
HPX_{MMP-2} + GM6001-X	10.00	0.040	0.0016	400
ProMMP-3	−	no binding		
MMP-3	−	0.022	0.0005	245
MMP-3 + GM6001-X	10.00	no binding		
MMP-3(ΔC)	−	0.021	0.0010	479
MMP-3(ΔC) + GM6001-X	10.00	no binding		
MT1-MMP(ΔC)	−	0.051	0.0034	677
MT1-MMP(ΔC) + GM6001-X	10.00	no binding		

the presence of GM6001-X, the affinity for MMP-2 reduced in a concentration-dependent manner so that at 10 μM GM6001-X, the affinity was identical to that for proMMP-2 and for HPX_{MMP-2} alone. These results indicate that the active site of MMP-2 makes a significant contribution to the enzyme−inhibitor complex, but when the active site of MMP-2 is blocked, the interaction with TIMP-4 is primarily through the HPX_{MMP-2} domain.

DISCUSSION

TIMP-4 Expression and Folding. While TIMP-4 has been expressed in mammalian cells (*11*), baculovirus (*21*), and *Pichia* (*58*), this is the first reported expression of full-length TIMP-4 in *E. coli* and folding of active protein from inclusion bodies.

In the final purification step, active TIMP-4 was separated from inactive TIMP-4 on a MMP-1(E200A) affinity resin. The inactive TIMP-4 underwent similar shifts in mobility upon reduction as was seen with the active inhibitor, indicating that it is likely that similar disulfide bonds have been formed in the active and inactive forms. MALDI and electrospray mass spectrometry indicated that this TIMP-4 fraction was inactive because of inappropriate processing, i.e., retaining its initiation Met residue or N-terminal acetylation. Such N-terminal modification is a well-known potential problem of overexpression in *E. coli*, but is of crucial importance to the expression of active TIMPs, since a free N-terminal Cys1 residue is essential for TIMP inhibition of MMPs. Various factors affect N-terminal processing of expressed proteins in *E. coli*, such as saturation of the bacterial methionine aminopeptidase machinery, the host genotype, and the nature of the amino acid residues following the initiation Met. Proteins with Cys residues following the initiation Met are poorly processed (*59*), and

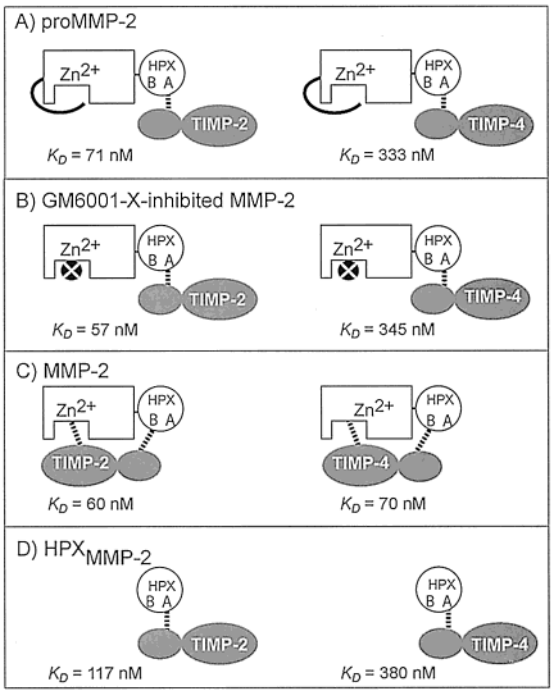

FIGURE 7: Schematic model showing mode of interaction of TIMP-2 and TIMP-4 with various forms of MMP-2. (A) TIMP-2 and TIMP-4 both bind to proMMP-2, although TIMP-2 has 4-fold higher affinity. This interaction is through the high affinity "A" site in the HPX$_{MMP-2}$ domain. (B) Binding of TIMP-2 and TIMP-4 to GM6001-X-inhibited MMP-2 resembles binding to proMMP-2. (C) TIMP-2 binding is insensitive to GM6001-X inhibition, while TIMP-4 affinity for MMP-2 is reduced 5-fold by GM6001-X treatment. This indicates that although TIMP-2 and TIMP-4 have similar affinity for MMP-2, the active site of MMP-2 contributes more to the overall free energy of binding to TIMP-4 than to TIMP-2. TIMP-2 and TIMP-4 interact with the both the catalytic domain and the putative low affinity "B" site of the HPX$_{MMP-2}$ domain. (D) Both TIMP-2 and TIMP-4 bind to HPX$_{MMP-2}$, but TIMP-2 interacts more strongly than TIMP-4.

interestingly, similar N-terminal processing problems have been reported for *E. coli* expressed TIMP-2 (*41*), which has the same N-terminal tripeptide sequence as TIMP-4. This inactive TIMP-4 may be useful as a negative control in future studies on TIMP-4 activity and biological functions as well as for dissecting the role of the C-terminal domain of TIMP-4 in various biological functions, such as inhibition of apoptosis (*25*, *60*). Our yield was about 10-fold lower than that previously achieved in either mammalian (*11*) or baculovirus (*21*) expression systems, indicating that those systems are more suitable for expression of TIMP-4. Alternatively, coexpression of TIMP-4 with methionine aminopeptidase (*61*) may improve the yield of active TIMP-4 from *E. coli*. Our current system, however, provided us with sufficient fully active TIMP-4 for detailed kinetic characterization and comparison with TIMP-1 and TIMP-2.

Kinetic Characterization. Published k_{on} values for TIMP inhibition of MMPs are generally in the range of 10^5-10^6 M^{-1} s^{-1}, with K_i values ranging from the high picomolar to low nanomolar range. We calculated K_i and k_{on} values for TIMP-1 inhibition to confirm the validity of our assay conditions, and these agree well with previously published data for TIMP-1 (*11*, *37*, *49*, *51*, *62*). Our data show that TIMP-4 is broadly similar to other members of the TIMP family in its inhibition of MMP-1, MMP-2, MMP-3, and MT1-MMP (Table 1). As is the case for TIMP-1 and TIMP-2, TIMP-4 reacts with MMP-2 20−60-fold faster than either MMP-1 or MMP-3. Our data for TIMP-4 inhibition of MMP-2 and MT1-MMP are in agreement with Bigg et al. (*11*) and extend the limited kinetic characterization of N-TIMP-4 of Stratmann et al. (*58*). TIMP-4 does not appear to differ markedly from other TIMPs in its inhibition of the tested MMPs, suggesting that its in vivo role is modulated by expression patterns and tissue localisation, as is the case with the other TIMPs. k_{on} values are higher and K_i lower for TIMP-1 and TIMP-4 inhibition of full-length MMP-1 and MMP-3 than for the catalytic domain alone, indicating that the C-terminal domains of the enzymes participate in binding to TIMP-4 (Table 1). K_{off} values were also determined directly using α_2M to irreversibly trap any MMP dissociating from MMP-TIMP complexes. For MMP-1 and MMP-3, the resultant k_{off} values agree well with those calculated from K_i and k_{on}. From Table 1, we predict that k_{off} for TIMP-4-MMP-2 is in the range of $\sim 1.5 \times 10^{-5}$ s^{-1}, which is about 5 times slower than that for MMP-1 and MMP-3. This suggests that we would be unable to calculate k_{off} using this method and, as expected, we saw no measurable dissociation over the time course of the experiment. The continuous nature of the assay described here does not permit monitoring for more than a few hours. Use of radiolabeled TIMP-4, as previously described for TIMP-2 (*63*), would permit direct calculation of this k_{off} value.

Inhibition of MMPs by TIMP was shown to be pH dependent, with K_i increased and k_{on} decreased by lowering pH (Table 2 and Figure 5). The pH profile of inhibition varies with the TIMP analyzed rather than the MMP, indicating that the effects observed are a result of protonation of the TIMP rather than the MMP. While our analysis does not permit identification of the residues involved, Cys1 of TIMP is known to be crucial for inhibition with its α-amino and carbonyl groups coordinating the catalytic Zn^{2+} ion of the MMP (*1*, *2*). The pK_a of the α-amino group of a half cystine residue is ∼7.9, and this value is normally reduced by about 1.5 units when the residue is at the N-terminus of a polypeptide chain. For TIMP-4, half-maximal k_{on} values are observed at pH 6.4, while for TIMP-1 and TIMP-2, half-maximal k_{on} values are observed at pH 7.4 and 7.0, respectively. These are within the expected pK_a values for an N-terminal half cystine, with slight variations between TIMPs, reflecting differences in their microenvironments. Furthermore, TIMP-4 retained low K_i values at more acidic pH values than either TIMP-1 or TIMP-2 (Table 2), indicating that TIMP-4 has inhibitory activity at more acidic pH values than TIMP-1 or TIMP-2. Since tumors are known to have lower extracellular pHs than surrounding normal tissues (*64*, *65*), TIMP-4 may have an extended protective effect against MMP activity compared with TIMP-1 or TIMP-2.

Mode of Binding of TIMP-4 and TIMP-2 to MMP-2. The IAsys biosensor system allowed us to investigate the mode of interaction of TIMPs with MMPs. TIMP binding to MMPs has been proposed to be a multistep process, involving both the catalytic and the HPX domains (*63*, *66*). However, in contrast with a previous report (*4*), a simple bimolecular model adequately described our data in all cases.

Our studies also indicate that TIMP-4 and TIMP-2 have similar affinities for MMP-2, but TIMP-4 has a 5-fold lower affinity for proMMP-2 and HPX$_{MMP-2}$ than TIMP-2. A

negatively charged stretch of amino acid residues (QEFLDIEDP) at the C-terminus of TIMP-2 plays an key role in TIMP-2 binding to proMMP-2 (*67*), with deletion of these nine residues reducing the k_{on} rate 4-fold (*51*). While the corresponding region in TIMP-4 (K**EF**V**DI**VQP) shares four identical residues (bold) and two conservative substitutions (underlined) out of nine residues (*10*), it is less negatively charged than the corresponding region of TIMP-2, having two acidic residues compared to four in TIMP-2. These differences may prevent TIMP-4 from forming strong electrostatic interactions with HPX_{MMP-2} and may underlie its inability to support ternary complex formation with MT1-MMP.

The observation that the low molecular weight inhibitor GM6001-X did not alter the affinity of TIMP-2 for MMP-2 is unexpected since, in most cases, the major binding energy for the formation of a protease-inhibitor complex is derived from the interaction with the active site of the enzyme. Indeed, the binding of other MMPs (MMP-1, -3, and -14) with TIMP-2 and TIMP-4 were completely blocked by GM6001-X. Therefore, the lack of hydroxamate effect on TIMP-2 binding to MMP-2 is unlikely to be an artifact. It is also unlikely that TIMP-2 is displacing GM6001-X from the MMP-2 active site given a vast excess of GM6001-X (K_i = 0.7 nM for inhibition of MMP-2) and a limited amount of TIMP-2. Even if GM6001-X were displaced by TIMP-2, its presence would reduce the apparent affinity between TIMP-2 and MMP-2, which we did not observe. In the presence of GM6001-X, the mode of interaction between MMP-2 and TIMP-2 is therefore considered to be similar to that between proMMP-2 and TIMP-2, being driven solely through HPX_{MMP-2} similar to the crystal structure of the TIMP-2-proMMP-2 complex with the inhibitory N-terminal domain of TIMP-2 exposed (*67*). Similarly, complex formation between TIMP-4 and the GM6001-X-inhibited MMP-2 is also through the C-terminal domains. Compared with TIMP-2, TIMP-4 has lower affinity for both the GM6001-X-inhibited form of MMP-2 and the HPX_{MMP-2}.

Although there was little difference in the K_D value between the GM6001-X-inhibited MMP-2 and the active MMP-2, for TIMP-2 binding, it is anticipated that a considerable energetic contribution is made through the interaction of the active site of the enzyme and the reactive site of the inhibitor. Therefore, we suspect that the interaction between HPX_{MMP-2} and the C-terminal domain of TIMP-2 is significantly reduced. This suggests that the mode of interaction through the two C-terminal domains in the proMMP-2-TIMP-2 complex (or the GM6001-X-inhibited MMP-2-TIMP-2 complex) is different from that in the MMP-2-TIMP-2 complex. Figure 7 depicts models for these differences. When the active site of MMP-2 is blocked either by the propeptide or GM6001-X, the high-affinity "A" site in the HPX_{MMP-2} is involved in TIMP-2 binding, whereas the low affinity "B" site is involved in the case of MMP-2-TIMP-2 complex. These two sites in HPX_{MMP-2} are also likely to be involved in interactions with TIMP-4.

The three-dimensional structure of the proMMP-2-TIMP-2 complex (*67*) suggests that activation of this complex, e.g., by a mercurial compound, 4-aminophenylmercuric acetate, must be accompanied by a considerable structural rearrangement in order for TIMP-2 to inhibit the activated MMP-2. We therefore postulate that the TIMP-2 binding site in proMMP-2 located between the third and fourth blades of HPX_{MMP-2} (illustrated as the "A" site) is different from the site that interacts with TIMP-2 in the active form ("B" site). Alternatively, "A" and "B" may reside in the same site of the HPX_{MMP-2} domain but the overall structural changes of MMP-2 upon binding to TIMP-2 (or TIMP-4) through the catalytic site may significantly lower the affinity between HPX_{MMP-2} and TIMP-2 (or TIMP-4). Clear understanding of how each domain of MMP-2 and TIMP-2 (or TIMP-4) interacts upon formation of the activated enzyme−inhibitor complex must await the determination of the three-dimensional structures of the MMP-2-TIMP-2 and MMP-2-TIMP-4 complexes.

REFERENCES

1. Brew, K., Dinakarpandian, D., and Nagase, H. (2000) *Biochim. Biophys. Acta 1477*, 267−283.
2. Gomis-Rüth, F. X., Maskos, K., Betz, M., Bergner, A., Huber, R., Suzuki, K., Yoshida, N., Nagase, H., Brew, K., Bourenkov, G. P., Bartunik, H., and Bode, W. (1997) *Nature 389*, 77−81.
3. Ogata, Y., Itoh, Y., and Nagase, H. (1995) *J. Biol. Chem. 270*, 18506−18511.
4. Olson, M. W., Gervasi, D. C., Mobashery, S., and Fridman, R. (1997) *J. Biol. Chem. 272*, 29975−29983.
5. Strongin, A. Y., Collier, I., Bannikov, G., Marmer, B. L., Grant, G. A., and Goldberg, G. I. (1995) *J. Biol. Chem. 270*, 5331−5338.
6. Butler, G. S., Butler, M. J., Atkinson, S. J., Will, H., Tamura, T., van Westrum, S. S., Crabbe, T., Clements, J., d'Ortho, M. P., and Murphy, G. (1998) *J. Biol. Chem. 273*, 871−880.
7. Kinoshita, T., Sato, H., Okada, A., Ohuchi, E., Imai, K., Okada, Y., and Seiki, M. (1998) *J. Biol. Chem. 273*, 16098−16103.
8. Toth, M., Bernardo, M. M., Gervasi, D. C., Soloway, P. D., Wang, Z., Bigg, H. F., Overall, C. M., DeClerck, Y. A., Tschesche, H., Cher, M. L., Brown, S., Mobashery, S., and Fridman, R. (2000) *J. Biol. Chem. 275*, 41415−41423.
9. Hernandez-Barrantes, S., Shimura, Y., Soloway, P. D., Sang, Q. A., and Fridman, R. (2001) *Biochem. Biophys. Res. Commun. 281*, 126−130.
10. Bigg, H. F., Shi, Y. E., Liu, Y. E., Steffensen, B., and Overall, C. M. (1997) *J. Biol. Chem. 272*, 15496−15500.
11. Bigg, H. F., Morrison, C. J., Butler, G. S., Bogeyevitch, M. A., Wang, Z., Soloway, P. D., and Overall, C. M. (2001) *Cancer Res. 61*, 3610−3618.
12. Stetler-Stevenson, W. G., Brown, P. D., Onisto, M., Levy, A. T., and Liotta, L. A. (1990) *J. Biol. Chem. 265*, 13933−13938.
13. Lotz, M., and Guerne, P. A. (1991) *J. Biol. Chem. 266*, 2017−2020.
14. Sato, T., Ito, A., Mori, Y., Yamashita, K., Hayakawa, T., and Nagase, H. (1991) *Biochem. J. 275*, 645−650.
15. Mann, J. S., Kindy, M. S., Edwards, D. R., and Curry, T. E., Jr. (1991) *Endocrinology 128*, 1825−1832.
16. Wick, M., Burger, C., Brusselbach, S., Lucibello, F. C., and Muller, R. (1994) *J. Biol. Chem. 269*, 18953−18960.
17. Greene, J., Wang, M., Liu, Y. E., Raymond, L. A., Rosen, C., and Shi, Y. E. (1996) *J. Biol. Chem. 271*, 30375−30380.
18. Leco, K. J., Apte, S. S., Taniguchi, G. T., Hawkes, S. P., Khohka, R., Schultz, G. A., and Edwards, D. R. (1997) *FEBS Lett. 401*, 213-217.
19. Tummalapalli, C. M., Heath, B. J., and Tyagi, S. C. (2001) *Cellular Biochemistry 80*, 512−521.
20. Dollery, C. M., McEwan, J. R., Wang, M., Sang, Q. A., Liu, Y. E., and Shi, Y. E. (1999) *Circ. Res. 84*, 498−504.
21. Liu, Y. E., Wang, M., Greene, J., Su, J., Ullrich, S., Li, H., Sheng, S., Alexander, P., Sang, Q. A., and Shi, Y. E. (1997) *J. Biol. Chem. 272*, 20479−20483.
22. Groft, L. L., Muzik, H., Rewcastle, N. B., Johnston, R. N., Knäuper, V., Lafleur, M. A., Forsyth, P. A., and Edwards, D. R. (2001) *Br. J. Cancer 85*, 55−63.
23. Hurst, D. R., Li, H., Xu, X., Badisa, L. D., Shi, Y. E., and Sang, Q. A. (2001) *Biochem. Biophys. Res. Commun. 281*, 166−171.
24. Hagemann, T., Gunawan, B., Schulz, M., Füzesi, L., and Binder, C. (2001) *Eur. J. Cancer 37*, 1839−1846.

25. Jiang, Y., Wang, M., Celiker, M. Y., Liu, Y. E., Sang, Q. X., Goldberg, I. D., and Shi, Y. E. (2001) *Cancer Res. 61*, 2365−2370.
26. Williamson, R. A., Carr, M. D., Frenkiel, T. A., Feeney, J., and Freedman, R. B. (1997) *Biochemistry 36*, 13822−13889.
27. Fernandez-Catalan, C., Bode, W., Huber, R., Turk, D., Calvete, J. J., Lichte, A., Tschesche, H., and Maskos, K. (1998) *EMBO J. 17*, 5238−5248.
28. Williamson, R. A., Muskett, F. W., Howard, M. J., Freedman, R. B., and Carr, M. D. (1999) *J. Biol. Chem. 274*, 37226−37232.
29. Tuuttila, A., Morgunova, E., Bergmann, U., Lindqvist, Y., Maskos, K., Fernandez-Catalan, C., Bode, W., Tryggvason, K., and Schneider, G. (1998) *J. Mol. Biol. 284*, 1133−1140.
30. Butler, G. S., Hutton, M., Wattam, B. A., Williamson, R. A., Knäuper, V., Willenbrock, F., and Murphy, G. (1999) *J. Biol. Chem. 274*, 20391−20396.
31. Chung, L., Shimokawa, K., Dinakarpandian, D., Grams, F., Fields, G. B., and Nagase, H. (2000) *J. Biol. Chem. 275*, 29610−26917.
32. Suzuki, K., Enghild, J. J., Morodomi, T., Salvesen, G., and Nagase, H. (1990) *Biochemistry 29*, 10261−10270.
33. Ogata, Y., Enghild, J. J., and Nagase, H. (1992) *J. Biol. Chem. 267*, 3581−3584.
34. Itoh, Y., Binner, S., and Nagase, H. (1995) *Biochem. J. 308*, 645−651.
35. Suzuki, K., Kan, C. C., Hung, W., Gehring, M. R., Brew, K., and Nagase, H. (1998) *J. Biol. Chem. 379*, 185−191.
36. Lichte, A., Kolkenbrock, H., and Tschesche, H. (1996) *FEBS Lett. 397*, 277−282.
37. Huang, W., Suzuki, K., Nagase, H., Arumugam, S., Van Doren, S. R., and Brew, K. (1996) *FEBS Lett. 284*, 155−161.
38. Kajita, M., Itoh, Y., Chiba, T., Mori, H., Okada, A., Kinoh, H., and Seiki, M. (2001) *J. Cell Biol. 153*, 893−904.
39. Grobelny, D., Poncz, L., and Galardy, R. E. (1992) *Biochemistry 31*, 7152−7154.
40. Bury, A. F. (1981) *J. Chromatogr. 213*, 491−500.
41. Wingfield, P. T., Sax, J. K., Stahl, S. J., Kaufman, J., Palmer, I., Chung, V., Corcoran, M. L., Kleiner, D. E., and Stetler-Stevenson, W. G. (1999) *J. Biol. Chem. 274*, 21362−21368.
42. Knight, C. G., Willenbrock, F., and Murphy, G. (1992) *FEBS Lett. 296*, 263−266.
43. Jeno, P., Mini, T., Moes, S., Hintermann, E., and Horst, M. (1995) *Anal. Biochem. 224*, 75−82.
44. Wilm, M., Shevchenko, A., Houthaeve, T., Breit, S., Schweigerer, L., and Fotsis, T. M. M. (1996) *Nature 379*, 466−469.
45. Shevchenko, A., Wilm, M., Vorm, O., and Mann, M. (1996) *Anal. Chem. 68*, 850−858.
46. Wait, R., Gianazza, E., Eberini, I., Sironi, L., Dunn, M., Gemeiner, M., and Miller, I. (2001) *Electrophoresis 22*, 3043−3052.
47. Vorm, O., and Mann, M. (1994) *J. Am. Soc. Mass Spectrom. 5*, 955−958.
48. Bieth, J. G. (1995) *Methods Enzymol. 248*, 59−84.
49. Nguyen, Q., Willenbrock, F., Cockett, M. I., O'Shea, M., Docherty, A. J. P., and Murphy, G. (1994) *Biochemistry 33*, 2089−2095.
50. Morrison, J. F., and Walsh, C. T. (1988) *Adv. Enzymol. Relat. Areas Mol. Biol. 61*, 201−301.
51. Willenbrock, F., Crabbe, T., Slocombe, P. M., Sutton, C. W., Docherty, A. J. P., Cockett, M. I., O'Shea, M., Brocklehurst, K., Phillips, I. R., and Murphy, G. (1993) *Biochemistry 32*, 4330−4337.
52. Aubry, M., and Bieth, J. (1976) *Biochim. Biophys. Acta. 438*, 221−230.
53. Ellis, K. J., and Morrison, J. F. (1982) *Methods Enzymol. 87*, 871−874.
54. Itoh, Y., Ito, A., Iwata, K., Tanzawa, K., Mori, Y., and Nagase, H. (1998) *J. Biol. Chem. 273*, 24360−24367.
55. Nagase, H., Itoh, Y., and Binner, S. (1994) *Ann. N.U. Acad Sci. 732*, 294−302.
56. Schuck, P. (1997) *Annu. Rev. Biophys. Biomol. Struct. 26*, 541−566.
57. Fujimoto, N., Ward, R., Shinya, T., Iwata, K., Yamashita, K., and Hayakawa, T. (1996) *Biochem. J. 313*, 827−833.
58. Stratmann, B., Farr, M., and Tschesche, H. (2001) *Biol. Chem. 382*, 987−991.
59. Hirel, P. H., Schmitter, M. J., Dessen, P., Fayat, G., and Blanquet, S. (1989) *Proc. Natl Acad. Sci. U.S.A. 86*, 8247−8251.
60. Jiang, Y., Goldberg, I. D., and Shi, Y. E. (2002) *Oncogene 21*, 2245−2252.
61. Hwang, D. D., Liu, L. F., Kuan, I. C., Lin, L. L., Tam, T. S., and Tam, M. F. (1999) *Biochem. J. 338*, 335−342.
62. Murphy, G., Allan, J. A., Willenbrock, F., Cockett, M. I., O'Connell, J. P., and Docherty, A. J. P. (1992) *J. Biol. Chem. 267*, 9612−9618.
63. Hutton, M., Willenbrock, F., Brocklehurst, K., and Murphy, G. (1998) *Biochemistry 37*, 10094−10098.
64. Webb, S. D., Sherratt, J. A., and Fish, R. G. (1999) *Clin. Exp. Metastasis 17*, 397−407.
65. Stubbs, M., McSheehy, P. M., Griffiths, J. R., and Bashford, C. L. (2000) *Mol. Med. Today 6*, 15−19.
66. Taylor, K. B., Windsor, L. J., Caterina, N. C. M., Bodden, M. K., and Engler, J. A. (1996) *J. Biol. Chem. 271*, 23938−23945.
67. Morgunova, E., Tuuttila, A., Bergmann, U., and Tryggvason, K. (2002) *Proc. Natl Acad. Sci. U.S.A. 99*, 7414−7419.

BI026454L